Extrapolation method for the no-core shell model

H. Zhan, A. Nogga, and B. R. Barrett
Department of Physics, University of Arizona, Tucson, Arizona 85721, USA

J. P. Vary
Department of Physics and Astronomy, Iowa State University, Ames, Iowa 50011, USA

P. Navrátil
Lawrence Livermore National Laboratory, L-414, P.O. Box 808, Livermore, California 94551, USA
(Received 11 August 2003; published 1 March 2004)

Nuclear many-body calculations are computationally demanding. An estimate of their accuracy is often hampered by the limited amount of computational resources even on present-day supercomputers. We provide an extrapolation method based on perturbation theory, so that the binding energy of a large basis-space calculation can be estimated without diagonalizing the Hamiltonian in this space. The extrapolation method is tested for ^{3}H and ^{6}Li nuclei. It will extend our computational abilities significantly and allow for reliable error estimates.

DOI: 10.1103/PhysRevC.69.034302 PACS number(s): 21.60.Cs, 21.10.Dr, 21.30.Fe, 24.10.Cn

I. INTRODUCTION

In recent years a great deal of progress has been made in solving the nuclear many-body problem based on microscopic nuclear interactions. Using a stochastic approach [1–3] or directly diagonalizing the Hamiltonian [4], previous investigations have been able to improve the accuracy of the calculations to a level, so that rather small parts of the Hamiltonian, such as the three-nucleon (3*N*) forces, can be probed by a comparison of the predicted spectra to the experimental values. For unambiguous conclusions, a reliable error bound for the calculations is of highest importance. Currently, error bounds have often been established using benchmark calculations [5,6,4,7]. In this paper, we propose a new scheme to extend no-core shell model (NCSM) calculations beyond their current limits, and to estimate error bounds for existing calculations. We establish a correlation between the expectation value of the Hamiltonian $\langle H\rangle$ with respect to the approximate ground state and that of the square of the Hamiltonian $\langle H^2\rangle$, following the ideas of Mizusaki and Imada [8,9]. This will improve the estimate of binding energies and provide more reliable error estimates.

To this aim, we proceed with a brief introduction to the main concepts of NCSM calculations in Sec. II. Then we motivate the correlation by the properties of NCSM effective interactions and perturbation theory in Sec. III. A comparison between the extrapolated results and the known binding energies for ^{3}H and ^{6}Li is given in Sec. IV. Conclusions and outlooks to the applications of this method and a discussion of the relation of this work to previous ones in Refs. [8,9] are presented in Sec. V.

II. NO-CORE SHELL MODEL

Usually shell-model calculations assume an inert nuclear core. Taking only the valence nucleons as active particles clearly has the advantage of reducing the number of many-nucleon states. But, so far, this also means that effective shell-model interactions have to be used, which cannot simply be related to nucleon-nucleon (*NN*) interactions, as they have been developed for few-nucleon systems.

The NCSM approach is different. All nucleons are taken to be active, and the same interactions are used as they are in traditional few-body methods. The calculations are performed in a finite antisymmetrized harmonic oscillator (HO) basis, using either Jacobi [10] or Cartesian coordinates such as those in usual shell-model investigations. In general, the short range repulsion of nuclear forces cannot be easily described in a finite basis. In particular, the HO basis is not well suited to describe the short range correlations and, on the other hand, the exponential tail of bound-state wave functions. Consequently, effective interactions appropriate to the basis-size truncation must be derived from the underlying nuclear forces in order to achieve convergence with a manageable number of basis states. These effective interactions can be systematically related to the "bare" *NN* interactions [7,11–13]. The scheme described in Refs. [7,12,13] is based on unitary transformations of the Hamiltonian [14], which decouple the model space from the complete Hilbert space describing the quantum mechanical system.

The starting point of all NCSM calculations is a nonrelativistic *A*-body Hamiltonian, which includes two-body interactions. The extension to 3*N* forces has been introduced in Refs. [15,16]. We do not take them into account in this study. Adding the center-of-mass (c.m.) HO potential, which is subtracted at a later stage in the calculation, one can cast the Hamiltonian [17] into the form

$$H_A^{\Omega}=\sum_{i=1}^{A}\left(\frac{\vec{p}_i^{\,2}}{2m_i}+\frac{m_i\Omega^2}{2}\vec{r}_i^{\,2}\right)+\sum_{i<j=1}^{A}\left(V_{ij}-\frac{m_i m_j}{2M_A}\Omega^2(\vec{r}_i-\vec{r}_j)^2\right), \tag{1}$$

where $\vec{p}_i(\vec{r}_i)$ is the momentum (position) of the particle *i* with mass m_i and $M_A=\Sigma_i m_i$ is the total mass of the *A* particles.

It is possible to establish a unitary transformation of the Hamiltonian, which decouples two parts of the Hilbert space—a rather small finite model space P and the rest of the Hilbert space Q. The projection operators on the two spaces are also called P and Q. They fulfill the relations $Q=1-P$, and $Qe^{-S}H_A^{\Omega}e^{S}P=0$, where e^{S} is the unitary transformation [7].

The solution of the A-body problem is made possible by the observation that, for nuclear problems, a cluster approximation to the full unitary transformation sufficiently speeds up the convergence compared to the bare interactions, so that practical calculations are possible. Instead of solving the full A-body problem, the procedure is carried out for a much smaller a-body problem, with $a=2$ or $a=3$ in practice. For such cases, one starts with the Hamiltonian

$$H_a^{\Omega}=\sum_{i=1}^{a}\left(\frac{\vec{p}_i^{\,2}}{2m_i}+\frac{m_i\Omega^2}{2}\vec{r}_i^{\,2}\right)+\sum_{i<j=1}^{a}\left(V_{ij}-\frac{m_i m_j}{2M_A}\Omega^2(\vec{r}_i-\vec{r}_j)^2\right). \tag{2}$$

Note that the mass of the full A-body system enters into the strength constant of the relative HO potential. Therefore, for this a-body Hamiltonian, the HO interaction does not cancel in the relative motion, and provides a confining mean-field interaction. However, the HO interaction is canceled in the A-body calculation. This procedure improves the convergence of our A-body results with increasing model space size.

Using the unitary transformation satisfying $Q_a e^{-S_a}H_a^{\Omega}e^{S_a}P_a=0$, one determines an effective Hamiltonian $H_{eff,a}^{\Omega}=P_a e^{-S_a}H_a^{\Omega}e^{S_a}P_a$, which exactly describes the a-body cluster in the model space. The truncation P_a from the full a-body Hilbert space is related to P by the requirement that the a-body states included in P are also included in P_a. One then defines the effective interaction to be used for the A-body calculation as

$$V_{eff,a}^{\Omega}=H_{eff,a}^{\Omega}-\sum_{i=1}^{a}\left(\frac{\vec{p}_i^{\,2}}{2m_i}+\frac{m_i\Omega^2}{2}\vec{r}_i^{\,2}\right). \tag{3}$$

With increasing size of the model space, the effective interaction converges to the bare interaction, so that the bare problem is recovered, meaning that the approximation is controllable.

Due to the cluster approximation, for $a<A$ we no longer have an exact effective interaction. This shows up, for example, in an Ω dependence of the binding energy. However, experience shows that shell-model calculations converge much faster, if performed with effective forces, as defined above [4]. All calculations in this paper are based on effective interactions obtained from two-body cluster solutions.

III. CORRELATION BETWEEN E_0 AND ΔE

The binding energy $E_0=\langle H\rangle$ evaluated for an approximate ground state must approach the exact binding energy $\mathcal{E}_0$ as the energy variance $\Delta E^2=\langle H^2\rangle-\langle H\rangle^2$ vanishes. One can easily extrapolate the exact binding energy with a series of approximate calculations, once the behavior of E_0 as a function of ΔE is determined. It is suggested by Mizusaki and Imada that E_0 can be expanded in terms of $\Delta E^2 E_0^{-2}$ for small values of $\Delta E^2 E_0^{-2}$ [8,9]. They propose two extrapolation formulas for traditional shell-model calculations: $E_0\simeq a\Delta E^2 E_0^{-2}+\mathcal{E}_0$ and $E_0\simeq a_0\Delta E^2+a_1\Delta E^4+\mathcal{E}_0$, where a, a_0, and a_1 are fitting parameters. This has motivated us to search for the correlation between E_0 and ΔE in context of the NCSM, and establish an extrapolation method for the NCSM.

A. Notation

For the following investigation we need to explicitly define the model spaces. To this aim, we truncate the full Hilbert space spanned by the antisymmetrized HO basis at a maximum total HO quantum number N_m. This N_m counts the number of oscillator quanta including the lowest oscillator configuration for the nucleus of interest [24]. This truncation ensures that all states are included up to a given energy, so that spurious c.m. motion can be projected out. The goal of the following study is to acquire results for a fixed N_m from calculations for even smaller subspaces $\widetilde{P}$ of P truncated by $\widetilde{N}_m\leqslant N_m$. The effective interactions will be obtained for the larger N_m in all cases.

We now switch to matrix notation, because it helps to demonstrate the structure of the effective Hamiltonian $\mathbf{H}$ which can be decomposed into

$$\mathbf{H}=\begin{bmatrix}\widetilde{\mathbf{H}} & \mathbf{B}\\ \mathbf{B}^{\mathrm{T}} & \hat{\mathbf{H}}\end{bmatrix}=\mathbf{H}_0+\mathbf{H}_1, \tag{4}$$

where

$$\mathbf{H}_0=\begin{bmatrix}\widetilde{\mathbf{H}} & \mathbf{0}\\ \mathbf{0} & \hat{\mathbf{H}}\end{bmatrix}\quad\text{and}\quad\mathbf{H}_1=\begin{bmatrix}\mathbf{0} & \mathbf{B}\\ \mathbf{B}^{\mathrm{T}} & \mathbf{0}\end{bmatrix}. \tag{5}$$

The boundaries of the blocks in $\mathbf{H}$ are given by the truncation $\widetilde{N}_m$ of the subspaces $\widetilde{P}$. $\widetilde{\mathbf{H}}$ acts only in $\widetilde{P}$ and $\hat{\mathbf{H}}$ in the remainder space $P-\widetilde{P}$. Because the effective interactions and $\mathbf{H}$ are defined for the complete P space, $\widetilde{N}_m$ completely determines $\widetilde{\mathbf{H}}$, so one may write explicitly $\widetilde{\mathbf{H}}(\widetilde{N}_m)$. We assume that $\boldsymbol{\psi}$ and $\boldsymbol{\phi}$ are the eigenvectors of $\widetilde{\mathbf{H}}$ and $\hat{\mathbf{H}}$, respectively, i.e., $\widetilde{\mathbf{H}}\psi_i=E_i\psi_i, i=0,\ldots,\tilde{n}-1$ and $\hat{\mathbf{H}}\phi_j=U_j\phi_j, j=0,\ldots,\hat{n}-1$, where $\tilde{n}$ and $\hat{n}$ are the dimensions of $\widetilde{P}$ and $P-\widetilde{P}$, respectively. Then the eigenvectors of $\mathbf{H}_0$ are

$$\mathbf{A}=\begin{bmatrix}\boldsymbol{\psi} & \mathbf{0}\\ \mathbf{0} & \boldsymbol{\phi}\end{bmatrix} \tag{6}$$

because of the form of $\mathbf{H}_0$. The ground state of $\mathbf{H}_0$, i.e., A_0, is of the from $[\psi_0^{\mathrm{T}},0]^{\mathrm{T}}$, and we denote the ground-state energy by E_0.

The energy dispersion ΔE is defined as

$$\Delta E^2=A_0^{\mathrm{T}}\mathbf{H}^2A_0-(A_0^{\mathrm{T}}\mathbf{H}A_0)^2=\psi_0^{\mathrm{T}}\mathbf{B}\mathbf{B}^{\mathrm{T}}\psi_0, \tag{7}$$

where we have made use of the specific forms of $\mathbf{H}_0$ and $\mathbf{H}_1$. The quantity ΔE^2 measures how well A_0 approximates the ground state of $\mathbf{H}$. As $\widetilde{N}_m$ approaches N_m, ΔE will vanish,

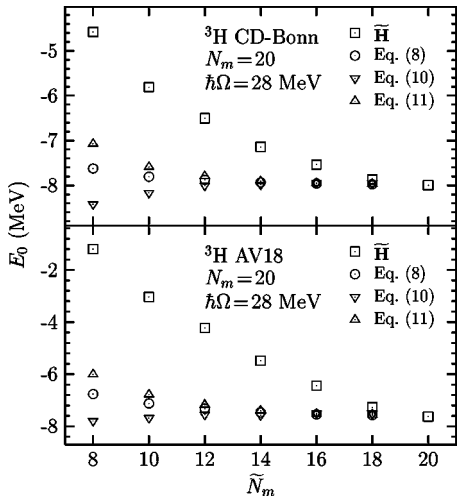

FIG. 1. Perturbative calculations of the binding energy E_0 of the triton with $N_m=20$ and $\hbar\Omega=28$ MeV. The values of E_0 for $\widetilde{\mathbf{H}}$ are denoted by open squares. The circles are calculated using Eq. (8), the downward triangles Eq. (10), and the upward triangles Eq. (11).

and E_0 will become the true binding energy $\mathcal{E}_0$.

To establish a scaling between E_0 and ΔE^2, we try to improve the results of $\widetilde{\mathbf{H}}$ using perturbation theory. Several more approximations will be necessary to motivate the scaling. These approximations will be tested numerically in model calculations for the ^{3}H binding energy. We do not intend to improve on the currently available ^{3}H binding energy results [1,18–20], but restrict ourselves to the P space truncated at $N_m=20$, which yields realistic but not fully converged results. Here we will only aim to recover P-space results with $\widetilde{N}_m<20$ calculations. Note that this is in contrast to the usual NCSM calculations where one investigates the dependence on N_m itself, and the effective interactions are renormalized for each N_m. This also means that our results will explicitly depend on Ω. But the small model space sizes used will allow us to extract intermediate results, which will demonstrate the origin of the scaling behavior. We will also show results for ^{6}Li to demonstrate the applicability to more complex systems.

B. Application of perturbation theory

With the block-block decomposition Eq. (4), second-order perturbation theory gives the eigenenergy of $\mathbf{H}$, i.e., $\mathcal{E}_i$, corresponding to E_i, as

$$\mathcal{E}_i \simeq E_i + \sum_{j=0}^{\hat{n}-1} \frac{(\psi_i^{\mathrm{T}}\mathbf{B}\phi_j)^2}{E_i - U_j}, \quad i=0,\ldots,\tilde{n}-1. \tag{8}$$

The next nonvanishing perturbative term is of the fourth order. Despite its simplicity and accuracy (see Fig. 1), Eq. (8) is not useful in establishing a correlation between E_0 and ΔE, because it requires the knowledge of all the eigenvalues and eigenvectors of $\hat{\mathbf{H}}$.

One may avoid diagonalizing $\hat{\mathbf{H}}$ by a redefinition of the decomposition,

$$\mathbf{H}_0 = \begin{bmatrix} \widetilde{\mathbf{H}} & \mathbf{0} \\ \mathbf{0} & \mathbf{D} \end{bmatrix} \quad \text{and} \quad \mathbf{H}_1 = \begin{bmatrix} \mathbf{0} & \mathbf{B} \\ \mathbf{B}^{\mathrm{T}} & \mathbf{C} \end{bmatrix}, \tag{9}$$

where $\mathbf{D}$ is a diagonal matrix containing the diagonal elements of $\hat{\mathbf{H}}$ and $\mathbf{C}=\hat{\mathbf{H}}-\mathbf{D}$. For NCSM Hamiltonians, this decomposition is appropriate (see Sec. III C). We note that Eq. (7) remains unchanged. Similar to Eq. (8), second-order perturbation theory gives

$$\mathcal{E}_i^{(2)} = E_i + \sum_{j=0}^{\hat{n}-1} \frac{(\psi_i^{\mathrm{T}}B_j)^2}{E_i - D_{jj}}, \quad i=0,\ldots,\tilde{n}-1, \tag{10}$$

where B_j is the jth column of $\mathbf{B}$. Up to the third order, we have

$$\mathcal{E}_i \simeq \mathcal{E}_i^{(2)} + \sum_{j,l=0}^{\hat{n}-1} \frac{(\psi_i^{\mathrm{T}}B_j)C_{jl}(B_l^{\mathrm{T}}\psi_i)}{(E_i - D_{jj})(E_i - D_{ll})}. \tag{11}$$

Figure 1 shows the binding energy of ^{3}H calculated using Eqs. (8), (10), and (11), and compares them to the results from the diagonalization of $\widetilde{\mathbf{H}}$. This is done for two different nuclear interactions, CD Bonn [21] and AV18 [22], using a Jacobi basis. This basis is obtained from the eigenstates of the antisymmetrizer (see Ref. [10]). The antisymmetrized states have a well-defined total quantum number N. Within each group of equal N, the states are ordered arbitrarily. Terms acting on the c.m. do not contribute in this case. It is seen that the perturbative calculations can greatly improve small $\widetilde{N}_m$ results, regardless of the choice of the nuclear interaction. Figure 1 also indicates that the third-order term in Eq. (11) is small for $\widetilde{N}_m>12$. This suggests that the nondiagonal matrix elements of $\hat{\mathbf{H}}$, i.e., $\mathbf{C}$, are small relative to their associated energy denominators in second-order perturbation theory.

C. E_0 vs ΔE^2 scaling

The expected scaling behavior can be motivated by considering the features and results of Eqs. (10) and (11). To this aim, the behavior of D_{jj} has to be understood in more detail. Figure 2 shows the matrix elements of the effective two-body Hamiltonian and the effective two-body kinetic energy for our triton model both in the 3N basis. The effective kinetic energy is calculated in the same way as the effective Hamiltonian, except that the NN interaction is turned off. In this case, the CD-Bonn potential is used with $N_m=20$ and $\hbar\Omega=28$ MeV. Comparing the kinetic energy with the full Hamiltonian, one sees that the kinetic energy dominates over the contributions from the NN interaction, especially for large HO quantum numbers. In the figure, the basis states are ordered according to their total HO quantum number N. The ordering within each of these groups is arbitrary.

The potential energy affects mostly the low-N states and cross terms among low-N states and high-lying states. The diagonal elements of the Hamiltonian are dominant over off-diagonal elements, which confirms our expectation. It is also striking that a large number of the diagonal elements are roughly equal. The dark blocks next to the diagonals of the

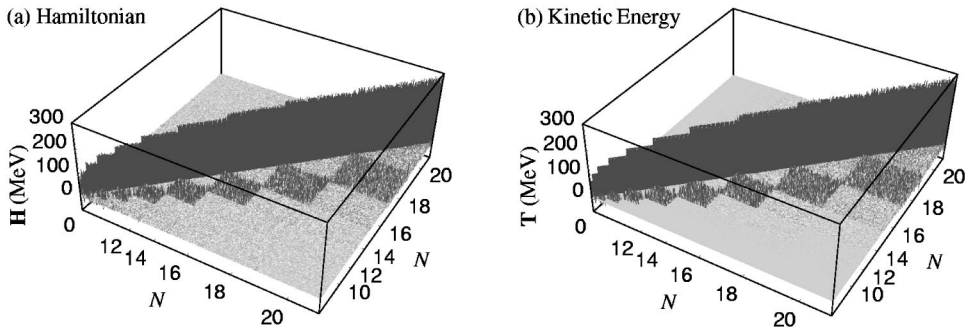

FIG. 2. (a) The effective Hamiltonian of the triton with the CD-Bonn potential and $\hbar\Omega = 28$ MeV. The basis is sorted according to the quantum number N, but the ordering within each group of states with the same N is arbitrary. This ordering will be assumed in all the following figures. (b) The effective kinetic energy, which is calculated in the same way as the Hamiltonian but with the *NN* interaction turned off.

Hamiltonian and the kinetic energy are due to the fact that the kinetic energy operator changes the quantum number N by ± 2 (also 0, which corresponds to the low-amplitude diagonal blocks). Since everything is renormalized to effectively include the higher-space ($N > N_m$) influence, $N \pm 4, \pm 6, \ldots$ terms show up in the Hamiltonian and the kinetic energy, and they become progressively weaker towards low N. The above properties persist for other interactions and other values of Ω or N_m. They are a common feature of NCSM effective Hamiltonians, at least for the $3N$ system.

The behavior of the diagonal matrix elements is quantified in Fig. 3. The upper panel shows individual diagonal elements, and, again, the basis states are ordered according to their HO quantum number. The lower panel plots the averages of the diagonal elements that have equal N. The step structure among the individual diagonal elements reflects the fact that D_{jj} is roughly the same in each group of states with the same HO quantum number. The reason for the flattening for larger N is twofold. First, the number of states increases dramatically for larger N and, second, the renormalization of the effective matrix elements reduces large-N diagonal elements. This is seen by comparing the average effective kinetic energy (circles) with the bare kinetic energy (squares), which is the expectation value of the kinetic energy operator with respect to HO basis states. For $N \leqslant 14$, both follow the linear $[(N+3)/2]\hbar\Omega$ behavior as expected. For higher N, the effective kinetic energy turns flatter. The figure also compares the averaged diagonal elements of the full Hamiltonians (triangles) to those of the kinetic energy. This again demonstrates the dominance of the kinetic energy for $N > 0$. One can expect that the same behavior holds for more complex nuclei.

This structure of the effective Hamiltonian guarantees that the denominators of the second-order term in Eqs. (10) and (11) are, to a high accuracy, equal over a wide range of N. Thus, we have approximately

$$\mathcal{E}_0 \simeq E_0 - \frac{1}{\alpha}\sum_{j=0}^{\hat{n}-1}(\psi_0^{\mathrm{T}} B_j)^2 = E_0 - \frac{1}{\alpha}\psi_0^{\mathrm{T}}\mathbf{B}\mathbf{B}^{\mathrm{T}}\psi_0, \qquad (12)$$

where α is a positive constant. Since the absolute value of E_0 is much smaller than D_{jj}, the constant α should be roughly the average value of the diagonal elements with $N > \tilde{N}_m$. This also means that α^{-1} is only weakly dependent on E_0. Neglecting higher-order perturbative terms and taking a constant true binding energy $\mathcal{E}_0$, it follows that $E_0 \propto \Delta E^2$. This motivates a linear scaling behavior between E_0 and ΔE^2.

IV. APPLICATION OF THE EXTRAPOLATION

Now that the linear scaling between E_0 and ΔE^2 has been motivated, one can estimate the true binding energy $\mathcal{E}_0$ by a linear regression of E_0 and ΔE^2 which are calculated with

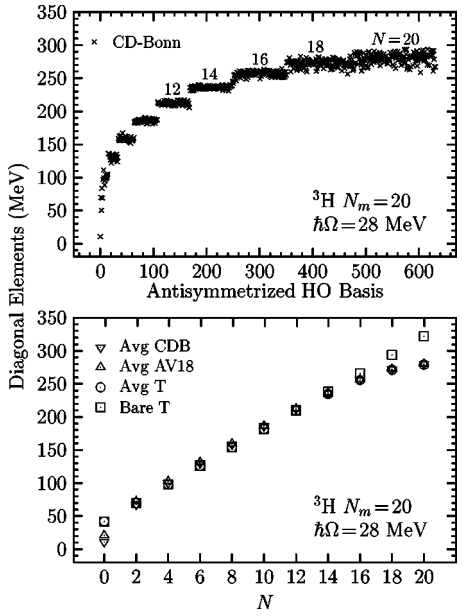

FIG. 3. The diagonal elements of the Hamiltonians and kinetic energies for ^{3}H. The horizontal axis in the upper panel enumerates the basis states for each individual diagonal element (crosses) of the model with the CD-Bonn potential. The horizontal axis in the lower panel indicates the HO quantum number N for other data. Bare T (squares) is the expectation value of the kinetic energy operator with respect to HO basis states. The remaining results are the averages of diagonal elements with the same HO quantum number N. From right to left, the first step of the individual diagonal elements in the upper panel corresponds to $N = 20$, the next $N = 18$, and so on.

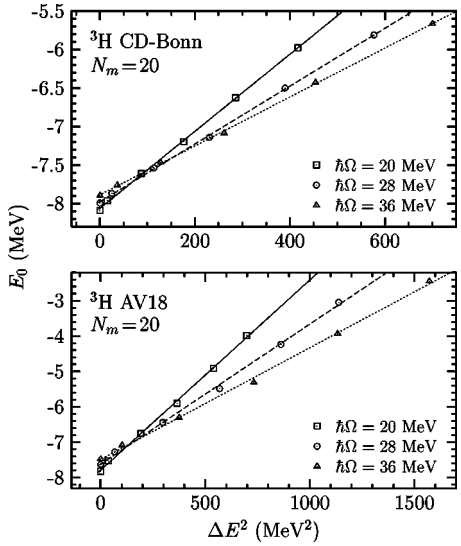

FIG. 4. The linear relation between E_0 and ΔE^2. The upper panel is for ^{3}H with the CD-Bonn potential, the lower one for AV18. Symbols from right to left correspond to $\widetilde{N}_m = 10, 12, \ldots, 20$ for each model. The lines fit the results from $\widetilde{N}_m = 10$ to 18.

$\widetilde{N}_m < N_m$, and extrapolating it to the point where $\Delta E^2 = 0$ to estimate $\mathcal{E}_0$ at N_m.

The numerical results for the relation between E_0 and ΔE^2 are shown in Fig. 4 for ^{3}H with different *NN* interactions and different values of $\hbar\Omega$. N_m is 20 in all cases and $\widetilde{N}_m$ varies between 10 and 20. Additionally, linear fits to the results for $\widetilde{N}_m = 10-18$ are plotted. Clearly, the linear scaling behavior is confirmed by these calculations.

To be more quantitative, we compare results of direct calculations, the extrapolation based on the scaling behavior, and perturbative estimates based on Eq. (11) in Table I. The table indicates the computational efforts necessary by giving run times for different calculations. One sees that a stable extrapolation is possible starting from $\widetilde{N}_m = 14$. The extrapolation error for larger calculations is comparable to the error of the perturbative estimates, indicating that both can be traced back to higher-order terms in the perturbative expansion. In calculations for $N_m = 30$, we have confirmed that the range of the linear behavior is extended for larger N_m. This is expected because $1/D_{jj}$ is driven by the kinetic energy and, therefore, is proportional to $1/N$ (see Fig. 3). Consequently, if N is increased by one step (i.e., 2 units), then the change in $1/D_{jj}$ is of the order of $1/N^2$, which decreases with N. We also note that the constant $\alpha = 268$ MeV for CD Bonn with $\hbar\Omega = 28$ MeV is comparable to the diagonal elements D_{jj} shown in Fig. 3.

TABLE II. Errors in perturbative estimates of the ^{3}H binding energy using Eqs. (8) and (10), and the difference between extrapolated binding energies and corresponding perturbative results from Eq. (10). All results are for CD-Bonn potential and $\hbar\Omega = 28$ MeV.

N_m	δE(Eq. [8])[a]	δE(Eq. [10])[a]	$\mathcal{E}_{0,\mathrm{e}} - \mathcal{E}_0^{(2)\mathrm{a,b}}$
8	87	119	−93
10	84	167	−12
12	40	60	−17
14	52	103	3
16	27	53	−12
18	29	64	3
20	13	39	−7

[a]Perturbative estimates are calculated with $\widetilde{N}_m = N_m - 2$. The results are in units of keV.
[b]$\mathcal{E}_{0,\mathrm{e}}$ is the extrapolated binding energy using only the results of E_0 and ΔE^2 from $\widetilde{N}_m = N_m - 2$ and $N_m - 4$.

The effect of N_m is demonstrated in Table II, where we list errors in perturbative estimates of the ^{3}H binding energy using Eqs. (8) and (10). The two equations are both of the second order, and the errors tend to decrease, though not monotonically, as the model space increases. At the same time, Table II shows that the extrapolated binding energies converge to the results of Eq. (10). This is expected, because our extrapolation method, i.e., Eq. (12), is based on an ap-

TABLE I. The ground-state energies E_0 of $\widetilde{\mathbf{H}}$ for ^{3}H, their deviation from the correct result δE, and the computational time necessary for the solution. The results of the small space ($\widetilde{\mathbf{H}}$) solution are compared to the extrapolation method and the perturbative calculation using Eq. (11). All results are for CD-Bonn potential and $\hbar\Omega = 28$ MeV.

	$\widetilde{\mathbf{H}}$			Extrapolation			Perturbation		
$\widetilde{N}_m$	E_0[a]	δE[b]	t[c]	E_0[a]	δE[b,d]	t[c]	E_0[a]	δE[b]	t[c]
12	−6.502	1493	8.2	−7.940	55	13	−7.793	202	12
14	−7.140	855	25	−8.015	−20	39	−7.906	89	28
16	−7.536	459	82	−7.980	15	120	−7.950	45	84
18	−7.869	126	210	−7.970	25	340	−7.968	27	210
20	−7.995	0	510						

[a]In units of MeV.
[b]$\delta E = E_0 - \mathcal{E}_0$, in units of keV.
[c]In units of t_8, the time needed to solve the ground state of $\widetilde{\mathbf{H}}$ with $\widetilde{N}_m = 8$.
[d]The extrapolation uses E_0 and ΔE^2 of $\widetilde{\mathbf{H}}(\widetilde{N})$ with $\widetilde{N}$ from 10 to $\widetilde{N}_m$.

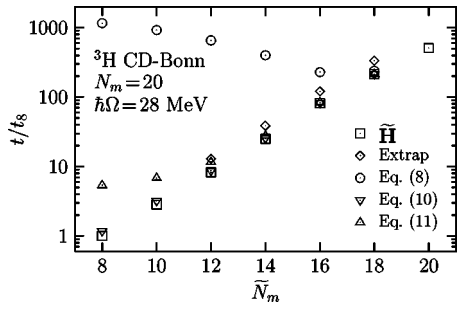

FIG. 5. The time consumed in the calculation in units of t_8, the time needed to solve the ground state of $\widetilde{\mathbf{H}}$ with $\widetilde{N}_m=8$. The diamonds mark the time it takes to extrapolate the ground state of $\mathbf{H}$ using all the ground states of $\widetilde{\mathbf{H}}(\widetilde{N})$ with $\widetilde{N}=10,\ldots,\widetilde{N}_m$, so it is the accumulation of the time needed to solve $\widetilde{\mathbf{H}}(\widetilde{N})$. All other symbols are as shown in Fig. 1.

proximation of second-order perturbation theory. The behavior of the perturbative calculations and extrapolations suggests that one can reduce the extrapolation error by increasing N_m.

The run times are also compared in Fig. 5. It is clear that perturbation theory based on Eq. (8) does not improve the timings because of the extra time needed to diagonalize $\hat{\mathbf{H}}$. The extrapolation method for $\widetilde{N}_m=14$ yields sufficiently accurate results, but reduces the CPU time by a factor of 13 compared to the full calculation. A similarly accurate perturbative calculation based on Eq. (11) is still eight times slower, which demonstrates the usefulness of the extrapolation to extend the calculations beyond their current limits.

We now apply the extrapolation method to the ^{6}Li nucleus. The numerical results have been obtained using the many-fermion dynamics code [23]. Since we work here in a basis of Slater determinants, we guarantee a 0*s* oscillator state of c.m. motion of our physical states by adding a c.m. term to Eq. (4), $\Lambda(\mathbf{H}_{\mathrm{c.m.}}-\frac{3}{2}\hbar\Omega)$ [7], with $\Lambda=10$. This separates excited states of c.m. motion from low-lying physical states. Figure 6 shows the results with $N_m=12$ (i.e., 10 $\hbar\Omega$ above the lowest unperturbed oscillator configuration of ^{6}Li [24]). The basis dimension of the $N_m=12$ calculations is 9.7 million, which is the largest model space published to date for ^{6}Li. This low value of N_m limits what $\widetilde{N}_m$ values one can

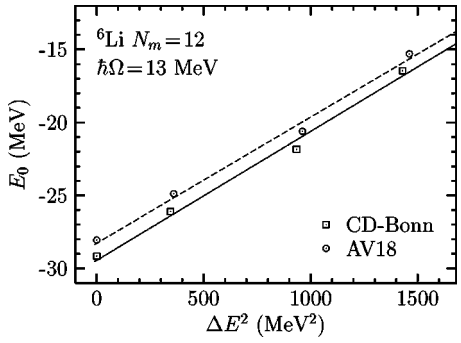

FIG. 6. The same as shown in Fig. 4, but for the ^{6}Li nucleus. Symbols from right to left correspond to $\widetilde{N}_m=6,8,10$, and 12 for each model. The lines fit the results from $\widetilde{N}_m=6,8$, and 10.

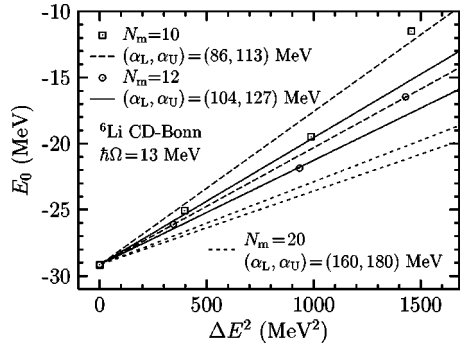

FIG. 7. The effect of N_m on the extrapolation error. Symbols from right to left correspond to $\widetilde{N}_m=N_m-6,\ldots,N_m$. The lines follow $E_0=\alpha_L^{-1}\Delta E^2+\mathcal{E}_0$ and $E_0=\alpha_U^{-1}\Delta E^2+\mathcal{E}_0$ for each N_m. The lines with $N_m=20$ are estimated from the effective kinetic energies.

use in the extrapolation for two reasons. First, the potential energy is not negligible at small quantum numbers, so $\widetilde{N}_m$ should be at least greater than four (the ground state of ^{6}Li has $N=2$). Second, the accuracy of the extrapolation depends on the dominance of the diagonal elements of $\mathbf{H}$, which is also weakened at small N. Thus, E_0 and ΔE^2 from $\widetilde{N}_m=4$ calculations are not in line with those from $\widetilde{N}_m=6,8,10$, and 12. The extrapolation errors are 290 keV (CD Bonn) and 220 keV (AV18). The CD-Bonn potential provides 1.1 MeV more binding than the AV18 potential. Thus, it is interesting to note that the difference between the two potentials is larger than the extrapolation error.

The range of $\widetilde{N}_m$ that is suitable for extrapolation is expected to increase with N_m. This is confirmed in Fig. 7, where an additional $N_m=10$ calculation is made for comparison. It is seen that the results are much more linear for the case $N_m=12$. Figure 7 also demonstrates why a higher value of N_m is likely to produce a smaller extrapolation error. We can estimate the lower and upper bounds of the constant α, (α_L,α_U), in Eq. (12) using effective kinetic energies and unperturbed ground-state energies E_0 for $\widetilde{N}_m=N_m-2$ and N_m-6. The results of $\widetilde{N}_m$ calculations are consistent with second-order perturbation theory, because they are roughly bounded by α_L and α_U for each N_m. The opening angle between the lines of slope α_L^{-1} and α_U^{-1} decreases as N_m increases. Hence, we expect to reduce the extrapolation error by increasing N_m.

V. CONCLUSIONS AND OUTLOOK

Because of the need for a large basis space to achieve accurate results, even light nuclei require a significant amount of computing resources to be investigated in the NCSM. We have justified and verified an extrapolation method for NCSM calculations. It is reliable, and can provide good estimates of large-space results from several small-space calculations. Sometimes, it may be the only means for getting a useful estimate of the NCSM result for otherwise unachievable large model spaces.

The extrapolation formula proposed in Ref. [9] agrees in

leading order with our Eq. (12). We would like to emphasize that the linear scaling between E_0 and ΔE^2 is based on perturbation theory. It is not an expansion in terms of $\Delta E^2 E_0^{-2}$ because ΔE^2 can be much greater than E_0^2 in the NCSM (see Fig. 4). The reasoning behind our extrapolation method is probably applicable only to NCSM calculations, because we have explicitly made use of the structure of the Hamiltonian in our derivation. The linear scaling between E_0 and ΔE^2 relies on the flattening of the diagonal elements of the effective Hamiltonian (dominated by the kinetic energy) as N approaches N_m. With this behavior, the energy denominator in Eq. (10) can be approximated by a constant α.

Generally speaking, extrapolation methods depend not only on the structure of a Hamiltonian but also on the truncation scheme that is used to produce an approximate state. Different truncation schemes may lead to different scaling behavior [9]. The traditional phenomenological shell model does not generate the structure of the Hamiltonian that is advantageous for our method. Specifically, in calculations with a core diagonal dominance is reduced since energies relative to a core are obtained. For realistic mean-field potentials, the single particle spectrum does not rise as fast as an oscillator spectrum which itself does not rise as fast as the kinetic spectrum in an oscillator basis. Hence, the diagonal dominance we have in the NCSM is much stronger than the traditional shell model, and our method probably cannot be applied to the traditional shell model without modifications. On the other hand, the methods for the traditional shell model do not necessarily apply to the NCSM either. In fact, it is evident from Fig. 6 that a quadratic fit [9] to the $\tilde{N}_m = 6, 8$ and 10 results will yield a significantly larger error.

From Table II we have learned that for small model spaces there are two competing sources of inaccuracy: one in the perturbation theory result and the other in the extrapolated result. We have shown that the extrapolated result is converging to the perturbation theory result, Eq. (10). In Table II one sees that the deviation of Eq. (10) and the extrapolation is already small even for relatively small values of N_m, e.g., $N_m = 10$. Since perturbation theory requires larger N_m, around 16, to give estimates of similar accuracy, we can conclude that overall our results are probably dominated by errors due to perturbation theory.

This method, such as NCSM calculations themselves, is limited by the size of the model space, because ΔE^2 has to be evaluated in the full P space. Nevertheless, it has been shown to be a valuable tool. Its power is based on the much smaller dimension of the **B** matrix compared to the full matrix for the Hamiltonian operator. Calculations for even larger model spaces will become possible once we make explicit use of the small dimension of the **B** matrix in our codes.

In Figs. 4 and 6, we observe that the extrapolation error, i.e., $\delta E = E_0 - \mathcal{E}_0$, at $\Delta E^2 = 0$ is quite small compared with differences in exact results of $\mathcal{E}_0$ for various values of $\hbar\Omega$ or choices of potentials. Therefore, the extrapolation can also serve as a way to estimate the uncertainties of NCSM results arising from $\hbar\Omega$ dependence and choices of interactions. This will be an important application of our method in future investigations of nuclei within the NCSM.

ACKNOWLEDGMENTS

H.Z., A.N., and B.R.B. acknowledge partial support by NSF grant No. PHY0070858. J.P.V. acknowledges partial support by U.S. Department of energy Grant No. DE-FG-02 87ER40371. This work was partly performed under the auspices of the U.S. Department of Energy by the University of California, Lawrence Livermore National Laboratory under Contract No. W-7405-Eng-48. This research used resources of the National Energy Research Scientific Computing Center, which is supported by the Office of Science of the U.S. Department of Energy under Contract No. DE-AC03-76SF00098.

[1] S. C. Pieper and R. B. Wiringa, Annu. Rev. Nucl. Part. Sci. **51**, 53 (2001).
[2] Y. Suzuki and K. Varga, *Stochastical Variational Approach to Quantum-Mechanical Few-Body Problems*, Lecture Notes in Physics Vol. m54 (Springer-Verlag, Berlin, 1998).
[3] S. E. Koonin, D. J. Dean, and K. Langanke, Phys. Rep. **278**, 1 (1997).
[4] P. Navrátil and W. E. Ormand, Phys. Rev. Lett. **88**, 152502 (2002).
[5] H. Kamada *et al.*, Phys. Rev. C **64**, 044001 (2001).
[6] B. R. Barrett, B. Mihaila, S. C. Pieper, and R. B. Wiringa, Nucl. Phys. News **13**, 20 (2003).
[7] P. Navrátil, J. P. Vary, and B. R. Barrett, Phys. Rev. C **62**, 054311 (2000).
[8] T. Mizusaki and M. Imada, Phys. Rev. C **65**, 064319 (2002).
[9] T. Mizusaki and M. Imada, Phys. Rev. C **67**, 041301(R) (2003).
[10] P. Navrátil, G. P. Kamuntavičius, and B. R. Barrett, Phys. Rev. C **61**, 044001 (2000).
[11] K. Suzuki and S. Y. Lee, Prog. Theor. Phys. **64**, 2091 (1980).
[12] K. Suzuki, Prog. Theor. Phys. **68**, 246 (1982).
[13] P. Navrátil, J. P. Vary, and B. R. Barrett, Phys. Rev. Lett. **84**, 5728 (2000).
[14] S. Okubo, Prog. Theor. Phys. **12**, 603 (1954).
[15] P. Navrátil and W. E. Ormand, Phys. Rev. C **68**, 034305 (2003).
[16] D. Marsden, P. Navrátil, S. Coon, and B. Barrett, Phys. Rev. C **66**, 044007 (2002).
[17] H. J. Lipkin, Phys. Rev. **109**, 2071 (1958).
[18] D. C. J. Marsden, P. Navrátil, S. A. Coon, and B. R. Barrett, Phys. Rev. C **66**, 044007 (2002).
[19] A. Nogga, H. Kamada, W. Glöckle, and B. R. Barrett, Phys. Rev. C **65**, 054003 (2002).

[20] A. Nogga, A. Kievsky, H. Kamada, W. Glöckle, L. E. Marcucci, S. Rosati, and M. Viviani, Phys. Rev. C **67**, 034004 (2003).
[21] R. Machleidt, Phys. Rev. C **63**, 024001 (2001).
[22] R. B. Wiringa, V. G. J. Stoks, and R. Schiavilla, Phys. Rev. C **51**, 38 (1995).
[23] J. P. Vary (unpublished); J. P. Vary and D. C. Zheng (unpublished).
[24] The quantum number N_m differs from "N_{max}" of Refs. [7,13] by the oscillator quanta of the lowest unperturbed oscillator configuration. Thus $N_m = N_{max}$ for ^{3}H, while $N_m = N_{max} + 2$ for ^{6}Li.